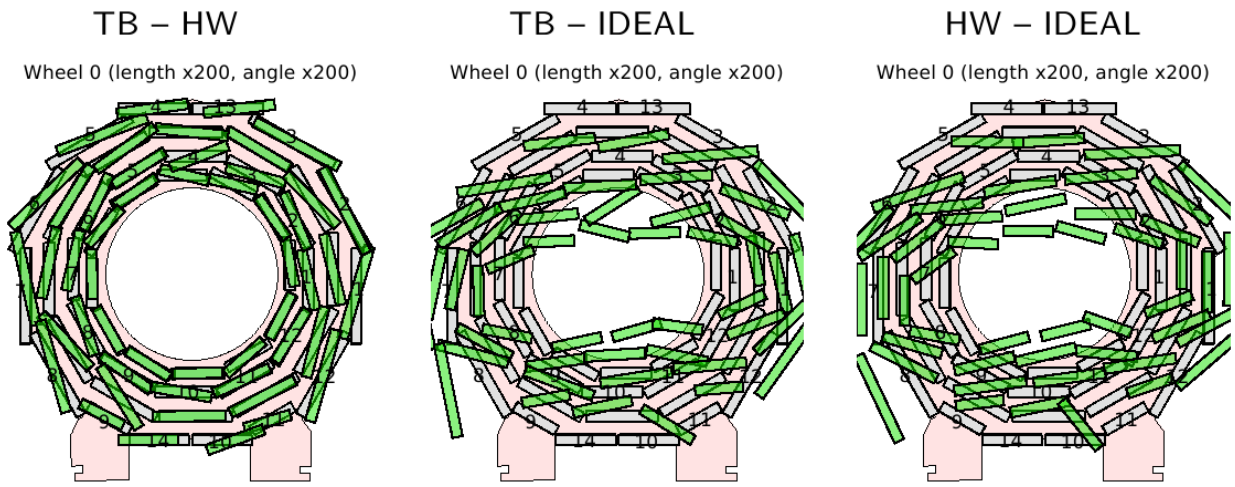

Figure 1: Exaggerated graphical view of differences between track-based (TB), hardware (HW), and unaligned (IDEAL) chamber positions and angles for wheel 0.

1 Quick introduction

This is a study of the effect of systematic alignment uncertainties on the shape of the $Z' \to \mu\mu$ peak. It is meant to be a first approximation of the Z' width uncertainty that feeds into limit-setting, though I'll point out some ways in which the study should be improved before it becomes a line in the systematics table of a Z' paper.

2 Current situation in muon alignment

We now have two independent measurements of the DT chamber positions: one from tracker-tracks propagated to the muon segments ("track-based alignment") and the other from in-situ physical measurements of the chamber positions, together with detailed studies of the internal chamber geometry from measurements at the construction sites to connect chamber positions to internal layer positions ("hardware alignment"). These two systems agree broadly about the cm-scale corrections that must be applied to the design geometry, mostly to account for gravitational sag (Fig. 1). However, mm-scale differences remain, and these differences have two systematic trends shown in Fig. 2: (1) groups of chambers in the same sector (ϕ-bin) appear to be coherently rotated such that wheel +2 chambers are displaced in one direction in $r\phi$ and wheel −2 chambers are displaced in the other direction in $r\phi$; (2) the two measurements differ in z-scale. Of these two effects, only the first ("twist") is relevant for momentum measurement and hence Z' resolution. The twist effect is shown more quantitatively in Fig. 3.

The same discrepancy has been studied at the level of raw residuals by plotting track residuals with the hardware geometry. This is equivalent to the chamber position comparison from the two alignments (Figs. 1–3), except that the binning is smaller than a chamber, the detector signals have are minimally processed (no multi-dimensional fits to all alignment degrees of freedom), and error bars are shown. A survey of $r\phi$ residuals versus z for station 1

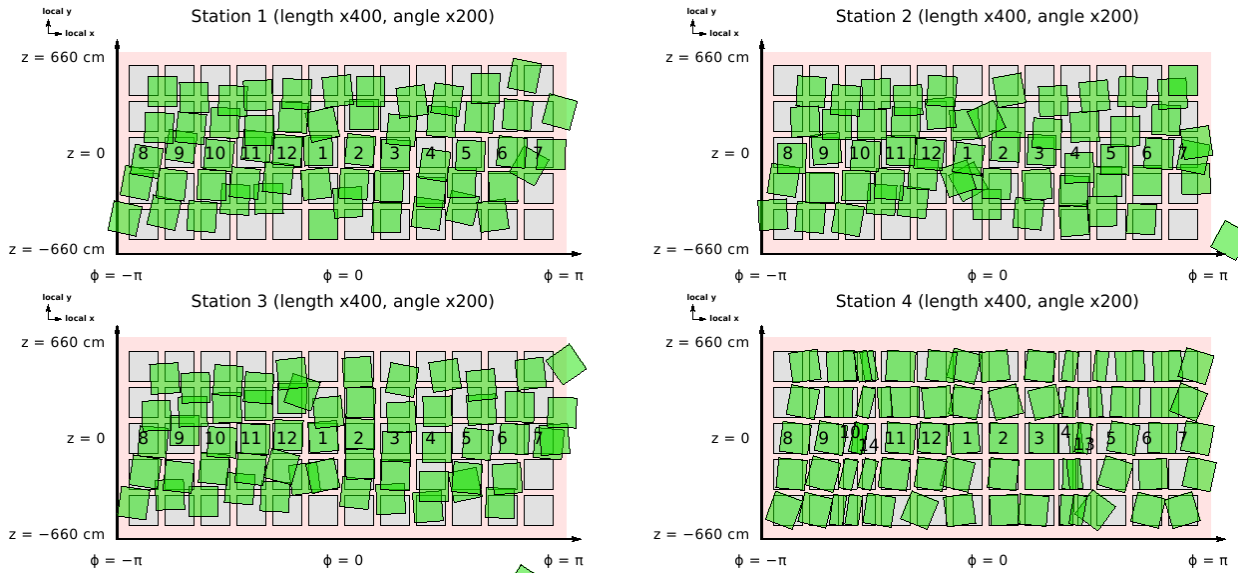

Figure 2: Exaggerated graphical view of differences between track-based and hardware geometries in the z-ϕ projection (unrolled muon barrel). Station 4 z positions cannot be measured by tracks (no z-measuring superlayer).

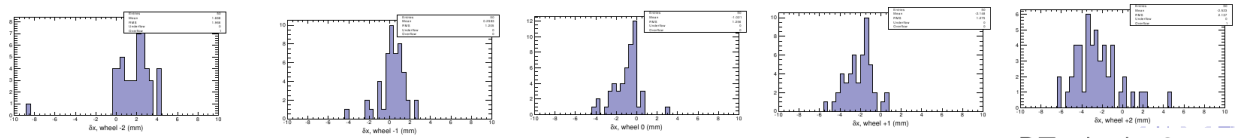

DT wheel -2
$\delta x = (1.7 \pm 2.0)$ mm

DT wheel -1
$\delta x = (0.3 \pm 1.2)$ mm

DT wheel 0
$\delta x = (-1.0 \pm 1.3)$ mm

DT wheel +1
$\delta x = (-2.2 \pm 1.3)$ mm

DT wheel +2
$\delta x = (-2.5 \pm 2.1)$ mm

Figure 3: Histogram of differences in chamber positions between track-based and hardware methods, separated by wheel. The "$(x \pm y)$ mm" numbers refer to the mean and RMS of each distribution.

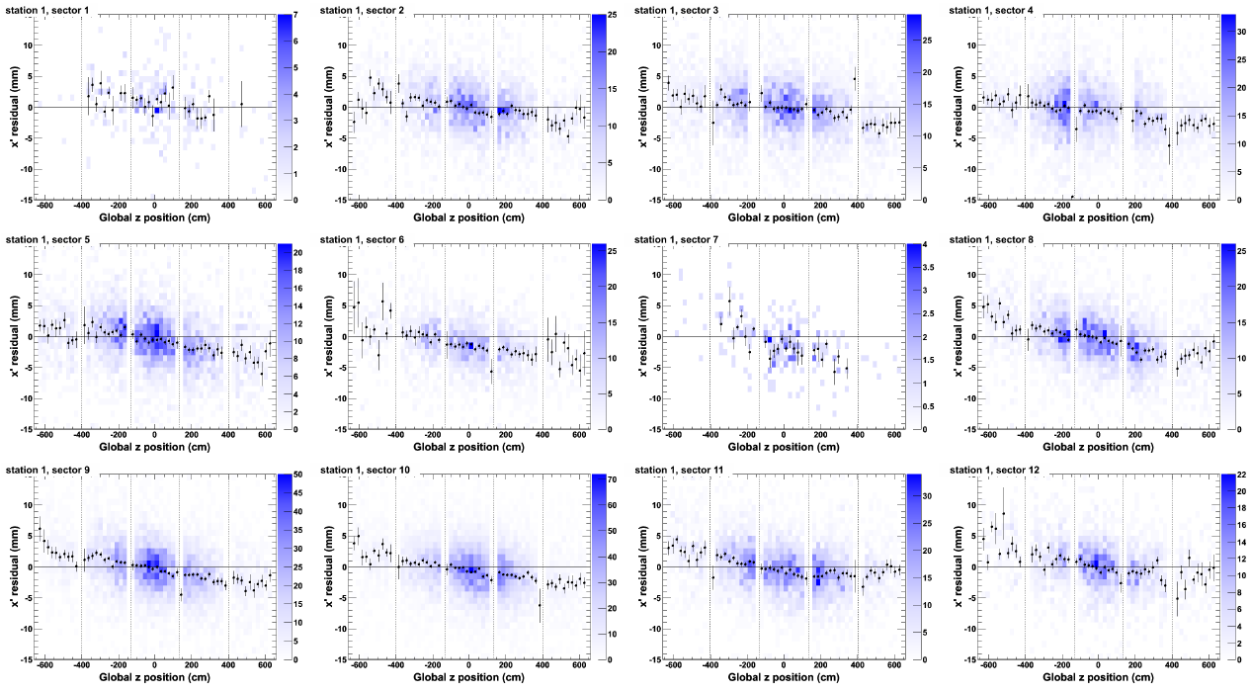

Figure 4: Global $r\phi$ residuals (also known as local x') versus global z position of the hit. The blue background is a 2-D distribution of the individual hits, the black points with error bars is the mean of each vertical slice, and the dashed lines indicate chamber boundaries (which are also wheel boundaries).

is presented in Fig. 4, illustrating the consistent "twist"-like slope of all 12 sectors.

To demonstrate the consistency of the effect for all sectors and all stations, the 12 plots in Fig. 4 and the 38 additional plots from stations 2–4 were fitted with a straight line: one example fit and the distribution of normalized χ^2 values are in Fig. 5. The slope of each fit characterizes the twist effect in that sector and station: histograms of all slopes are presented in Fig. 6, where we can see that they are clustered around -5×10^{-3} mm/cm, independent of station number.

The fact that these differences do not appear to grow with station number is significant because any bias in the propagated muon trajectory between the tracker and the muon chambers would yield differences that grow in proportion to the distance from the tracker. Station 4 is approximately twice as far from the tracker as station 1, but the effect in station 4 is clearly not twice the effect in station 1 (Fig. 6).

Many follow-up studies were performed, the most compelling of which is an measurement of the $+z$ and $-z$ ends of the barrel hardware system using 12 independent inclinometers (not used in the barrel fit), which measure changes in the angle of their installation relative to the direction of gravity. The inclinometer study confirms the hardware geometry as not being twisted. However, the fact that propagated tracks disagree with this geometry either means that a strange, non-growing tracking bias exists in the muon system or that the hardware geometry and inclinometers share a systematic uncertainty when propagated to layer positions. Either would be a problem for high-p_T tracking.

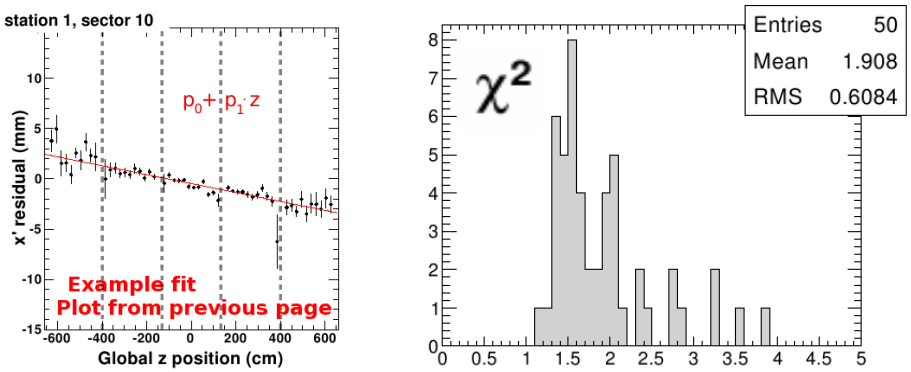

Figure 5: Left: example fit of one of the plots from Fig. 4. Right: distribution of $\chi^2/N_{\rm dof}$ for all such plots for all sectors, all stations. The $\chi^2/N_{\rm dof}$ values quantify the significance of hardware/track-based differences without the twist effect (deviations beyond the linear offset and slope).

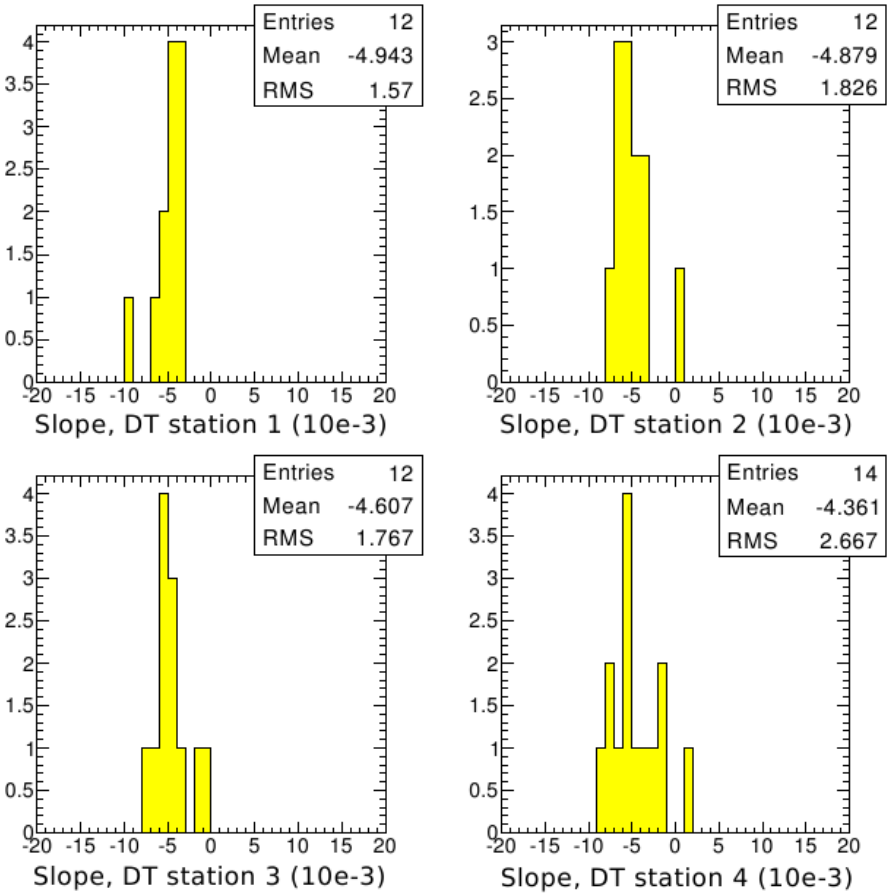

Figure 6: Slope of all fits from Fig. 5, demonstrating the lack of scaling with distance from the beamline. Slopes are expressed in units of 10^{-3} mm/cm (i.e. 10^{-4}).

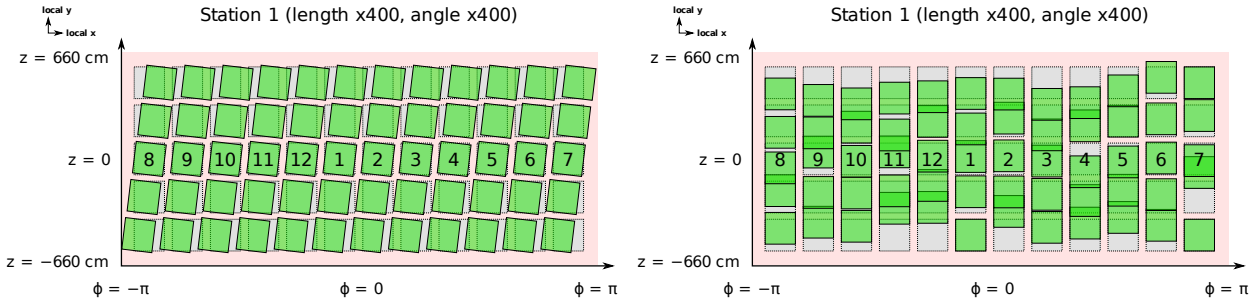

Figure 7: Exaggerated differences between "twist" (left) and "z-differences" (right) geometries and ideal, shown for station 1 in an unrolled-barrel view (compare with Fig. 2).

3 Studies of high-p_T resolution

Tracking biases in $r\phi$ directly impact track curvature measurements if the biased measurements have significant weight in the fit. Only very straight tracks ($p_T \gg 200$ GeV/c in the barrel) have a significant effective weight for muon hits in global muon track-fits due to the importance of long lever arms overwhelming the much higher intrinsic resolution of the tracker. In the high momentum limit, curvature biases in tracks $(q/{p_T}^{\text{measured}} - q/{p_T}^{\text{true}})$ are nearly proportional to hit position biases with a constant of proportionality of about 0.05 c/TeV per millimeter. Track-momentum biases will therefore be presented as curvature biases in units of c/TeV rather than momentum differences (GeV/c) or unitless ratios.

These studies were performed with three Z' samples with 1.1, 2, and 3 TeV/c^2 masses, respectively. Muons were refitted in the following four geometries:

- ideal: perfect alignment in Monte Carlo;
- twist: a 0.5 mrad rotation of sectors to match the magnitude of the track-based/hardware differences, systematic effect only (no random chamber-to-chamber variations);
- anti-twist: a -0.5 mrad rotation
- z-differences: track-based/hardware differences in the direction parallel with the beamline, no interference from other misalignment degrees of freedom.

The "twist" and "z-differences" geometries relative to ideal are presented in Fig. 7.

Improvement 1: re-reconstruct tracks from scratch with the new geometry, rather than using the track refitter.

Improvement 2: use standard Z' samples and resolution infrastructure, rather than the privately generated samples and ntuples that I used.

Figure 8 presents the first result: the effect of the twist on the GlobalMuon curvature measurement from a 1.1 TeV/c^2 Z'. Since the twist is a linear trend in $r\phi$ hit offsets versus z in the muon system, it causes a linear trend in curvature bias $(\kappa_{\text{refit}} - \kappa_{\text{gen}})$ versus η. (The proper abscissa to quantify a z-trend at a constant distance from the beamline is $\cot\theta$, but $\cot\theta = \eta + \mathcal{O}(\eta^3)$). The linear trend from the systematic misalignment has a comparable width to the intrinsic resolution seen in the ideal alignment. At $\eta = \pm 1$, there is an additional smearing due to tracks that cross the gap between the barrel and the endcap, since the endcap

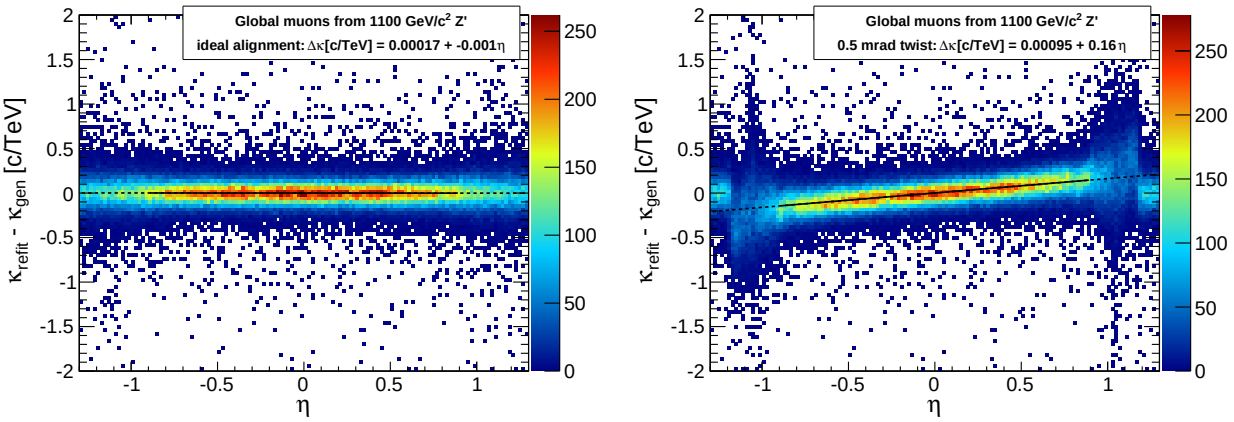

Figure 8: Curvature errors vs. η for a perfectly aligned system (left) and a muon system with a twisted barrel (right). The effect of the twist (linear trend) is comparable to the intrinsic momentum resolution (vertical spread). The artificial spread at $\eta = \pm 1$ is due to tracks that cross the gap between the coherently misaligned barrel and the perfectly aligned endcap.

was not misaligned. This is an artificial situation: the endcap will be aligned in a way that matches the barrel, and therefore this smearing is overly pessimistic.

Improvement 2: study the effect with the endcap twisted by the same amount as the barrel.

The effect of the twist behaves as expected when applied to higher-momentum muons or reversed (Fig. 9). Doubling the muon momentum increases the curvature bias only from 0.16 $c/\text{TeV}/\eta$ to 0.2 $c/\text{TeV}/\eta$, as it is approaching a constant bias in the high-momentum limit: see also Fig. 10. Reversing the twist of the underlying geometry reverses the slope of the curvature bias, demonstrating that it is a tunable parameter.

To quantify the effect on both p_T and η, curvature bias was plotted as a 2-D profile in Fig. 11. The dependence on p_T is approximately linear but not proportional, while the dependence on η is proportional. This is because it is a (very smooth, broad) threshold effect in p_T: when the sagitta of tracks is larger than the tracker measurements' resolution, the effective weight of the muon hits in the track-fit is negligible, and when the sagitta is much smaller than the tracker can measure by itself, the curvature bias is proportional to the hit-position bias and not the momentum of the track. This threshold is set by the radius and hit resolution of the tracker.

Finally, the effects on three TeV-muon reconstruction algorithms are compared in Fig. 12. The misalignment effect is largely independent of reconstruction algorithm.

4 Studies of η resolution

The track-based/hardware alignment discrepancies in the global z direction are also on the order of a few millimeters and significantly affect η reconstruction for TeV-scale muons. These errors in η negligibly affect Z' mass, as we will see in the next section.

The "z-differences" geometry prepared for this study includes both the systematic effect (z-length of the barrel) and the individual-chamber variations because the latter are evident

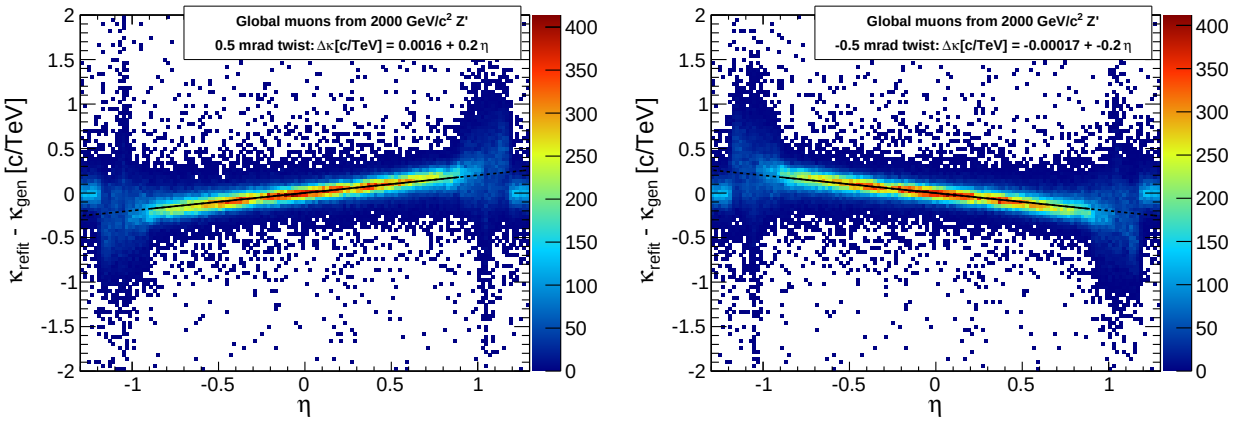

Figure 9: Curvature errors vs. η for muons from a 2 TeV/c^2 Z' in the twist geometry (left) and the anti-twist geometry (right).

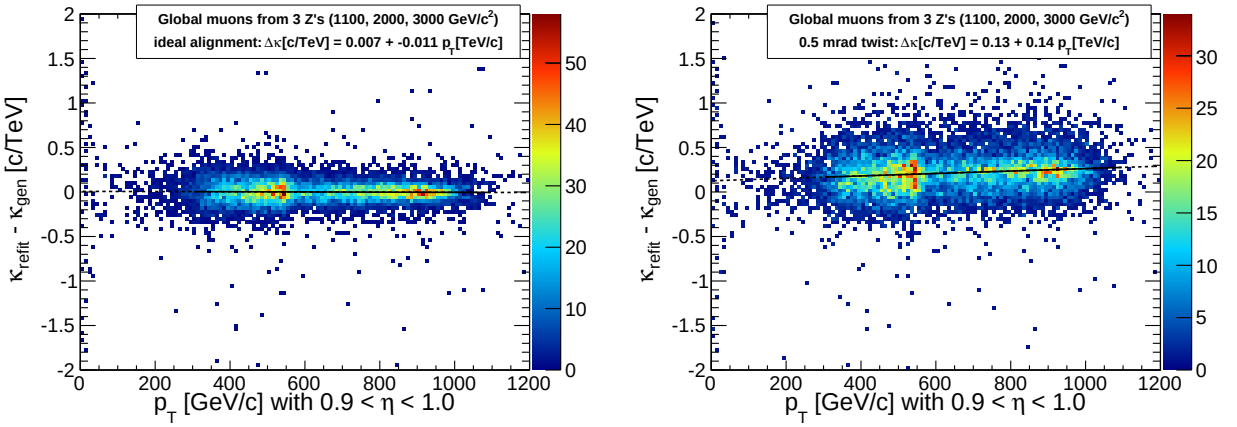

Figure 10: Curvature bias vs. p_T for muons from all three Z' samples (superimposed) in a slice of high η. Left: ideal geometry; right: twisted geometry. The effect is *not* proportional to p_T.

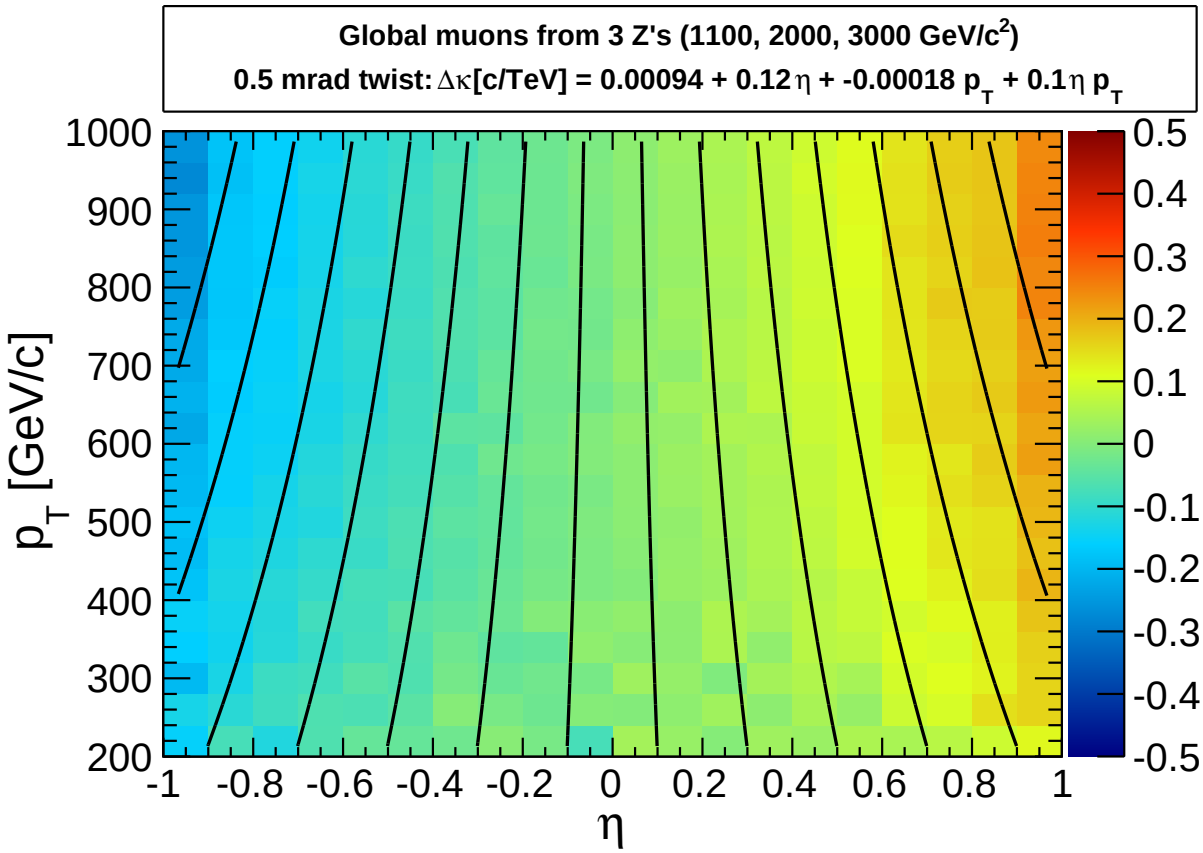

Figure 11: Curvature bias (color scale) vs. p_T and η with a 2-D fit represented by contour lines. The color of each pixel represents the mean curvature bias in that bin.

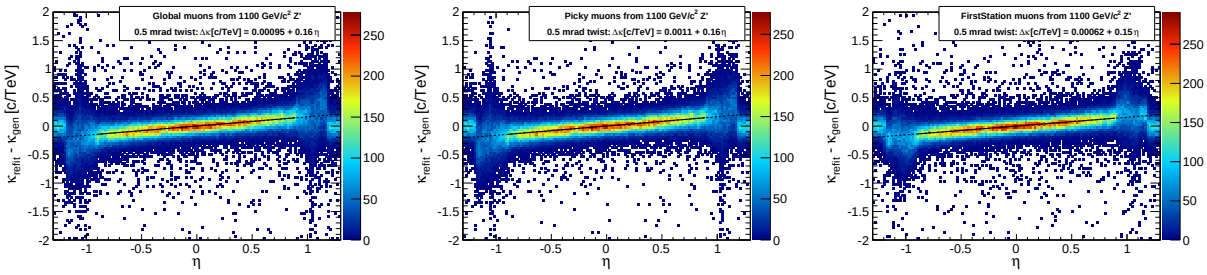

Figure 12: Curvature vs. η for GlobalMuons (left), the Picky track-fit (middle), and the FirstStation track-fit (right).

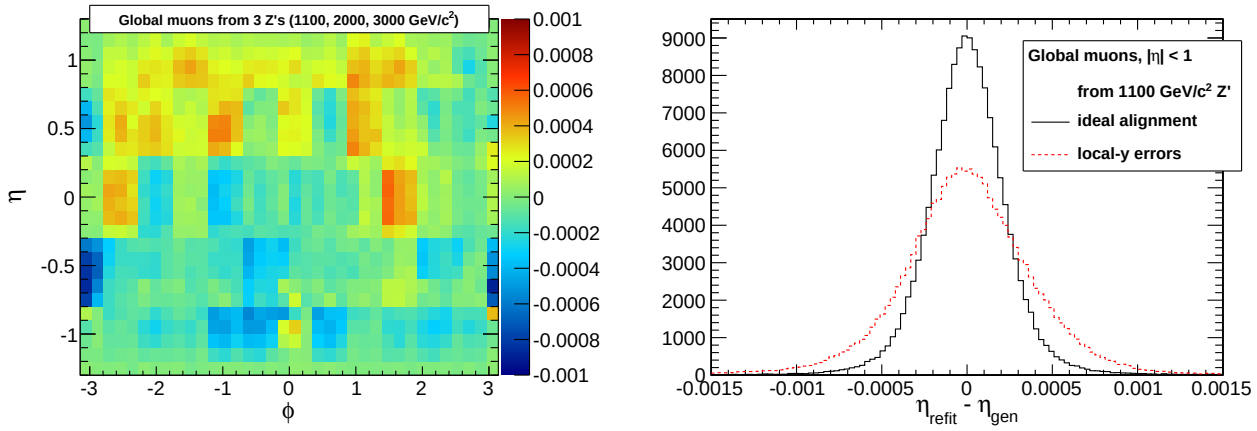

Figure 13: Left: $\eta^{\text{measured}} - \eta^{\text{true}}$ (color scale) in GlobalMuons from all three Z' samples vs. η and p_T. Right: histogram of $\eta^{\text{measured}} - \eta^{\text{true}}$ for the same samples, same geometry distortion.

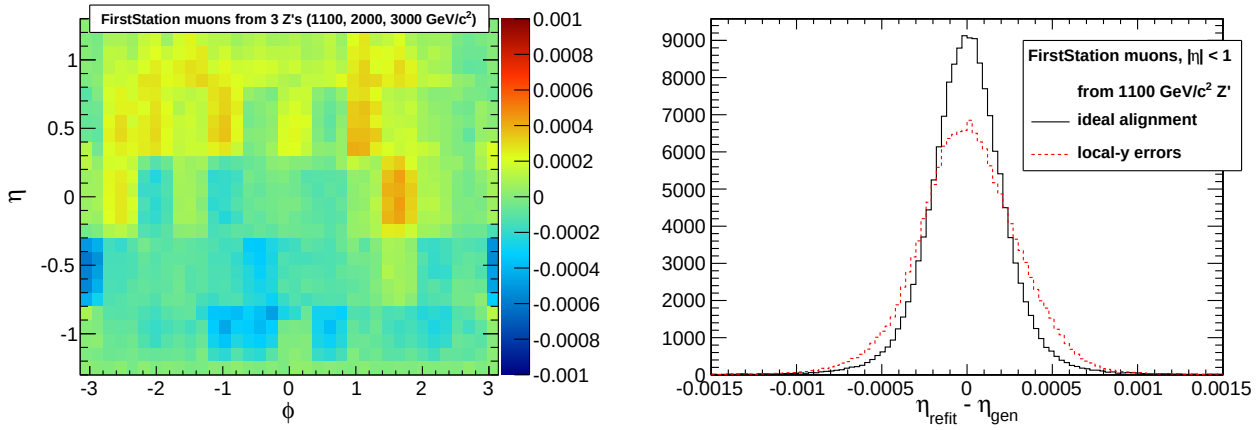

Figure 14: Left: $\eta^{\text{measured}} - \eta^{\text{true}}$ (color scale) in FirstStation from all three Z' samples vs. η and p_T. Right: histogram of $\eta^{\text{measured}} - \eta^{\text{true}}$ for the same samples, same geometry distortion.

in a plot of alignment residuals with sharp discrepancies at the boundaries (no long-distance propagation effect can account for discontinuities exactly at the chamber boundaries). Since the individual-chamber errors are in the model, we can see them in a plot of η bias as a function of η and ϕ, which maps the barrel in track-parameter bias (Fig. 13). The net effect of these misalignments smears the $\eta^{\text{measured}} - \eta^{\text{true}}$ distribution by 1×10^{-4}–1×10^{-3} (same Figure). Performing the same study with FirstStation refits instead of GlobalMuons (Fig. 14) reduces the bias and simplifies the η-ϕ map, since tracks are no longer being affected by muon chambers in different stations.

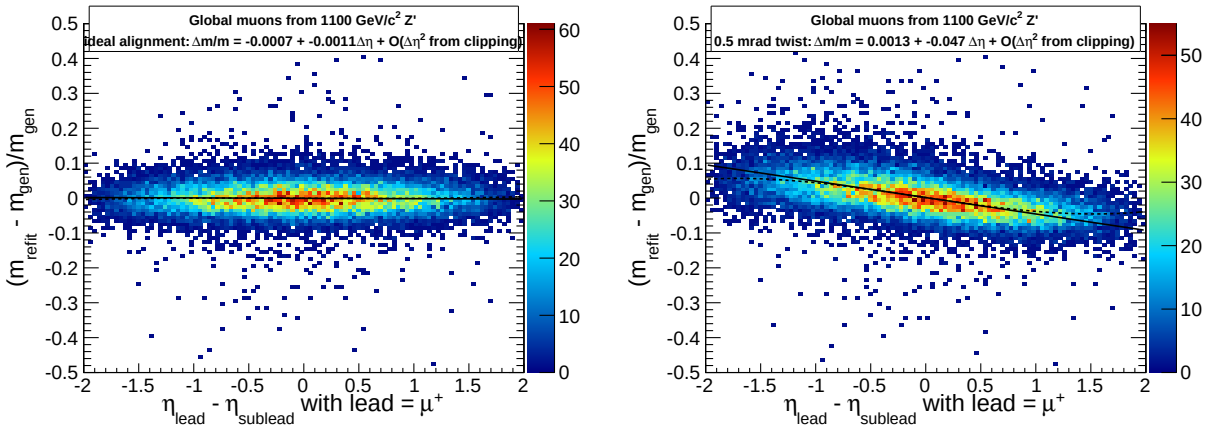

Figure 15: Mass bias vs. η difference of the daughters for events with μ^+ having the highest p_T (1.1 TeV/c^2 Z'); for each muon, we require $|\eta| < 1$. Left: ideal geometry; right: twist geometry.

5 Studies of Z' mass resolution

The bottom line for Z' studies is the mass resolution, which is most conveniently expressed as a percent: $(m^{\text{measured}} - m^{\text{true}})/m^{\text{true}}$. We want to see what effect the twist has on Z' mass thorugh momentum mismeasurement of its daughters, but the twist effect is highly dependent on η and the two muons may have very different η values. The most useful abscissa in this case is the η difference of the daughters, since the two muons encounter correlated effects that cancel in mass bias when they sample the detector at similar η values. More precisely, the mass bias is a function of

$$\Delta\eta = q_{\text{lead}} \left(\eta_{\text{lead}} - \eta_{\text{sublead}} \right)$$

Improvement 3: this should probably be $\eta_{\mu^+} - \eta_{\mu^-}$.

where "lead" and "sublead" refer to the highest-p_T and second-highest-p_T muons, respectively. Figure 15 shows the trend in mass bias due to a twist. Since only the barrel has been twisted, an $|\eta| < 1$ cut has been applied to each muon.

Improvement 4: $|\eta| < 1$ might not have been far enough: Fig. 8 shows that the tracks are already beginning to smear due to the artificial barrel-endcap mismatch by $|\eta| = 1$. Doing the study with continuity between the barrel and endcap would solve that problem.

The shape of the mass bias in Fig. 15 is not exactly linear, but it is approximately linear near $\Delta\eta \to 0$. The non-linear edges may be related to clipping the distribution with the $|\eta|$ cut on each muon, as illustrated in Fig. 16.

Figure 17 presents the effect of replacing the leading μ^+ muon with μ^-: the direction of the trend is reversed. Figure 17 shows the distribution with opposite twists: again, the direction is reversed. The twist parameter directly tunes the mass bias as a function of $\Delta\eta$.

Since Z' has a known η distribution, we can summarize the effect of the mass bias on the overall resolution of a Z' peak. This is shown in Fig. 19 for the 1.1, 2, and 3 TeV/c^2 Z' samples. The z-differences geometry has negligible effect on the Z' mass resolution because

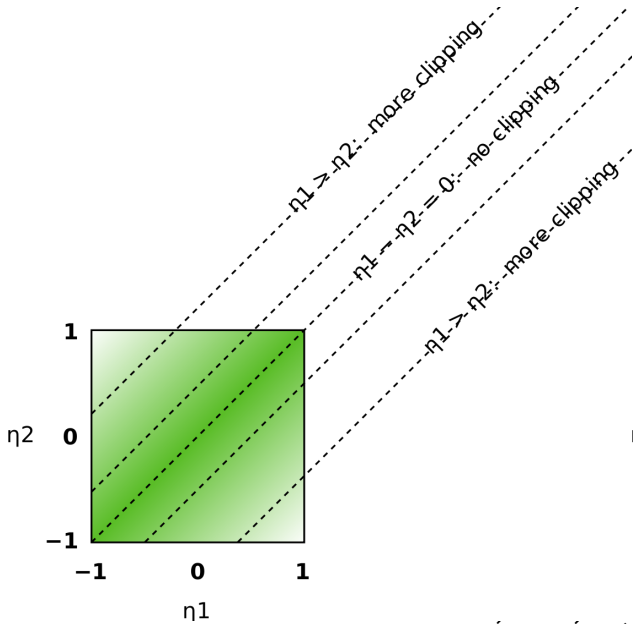

Figure 16: By applying an $|\eta| < 1$ cut on each muon, we sample a different distribution of the box as $\Delta\eta$ varies.

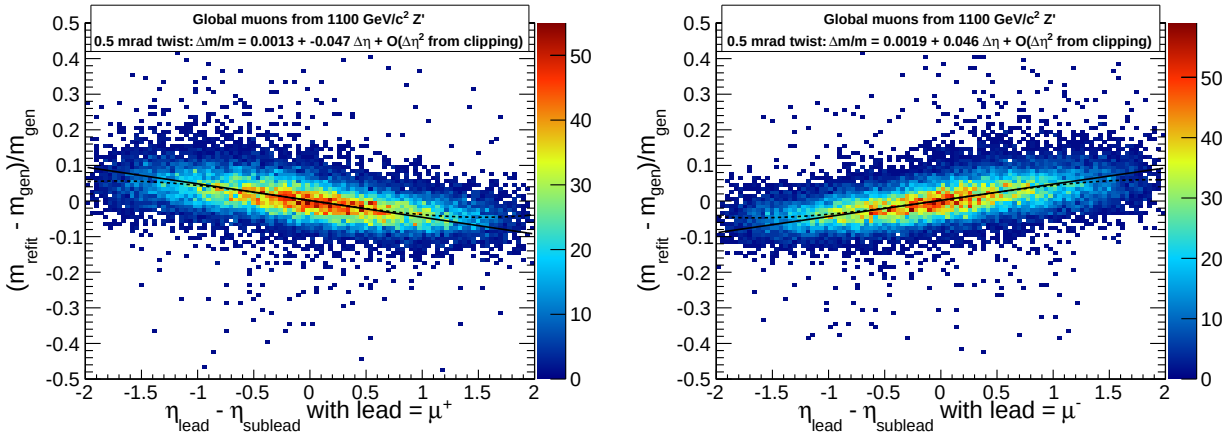

Figure 17: Mass bias vs. $\Delta\eta$ (1.1 TeV/c^2 Z') for μ^+ having the highest p_T (left) and μ^- having the highest p_T (right).

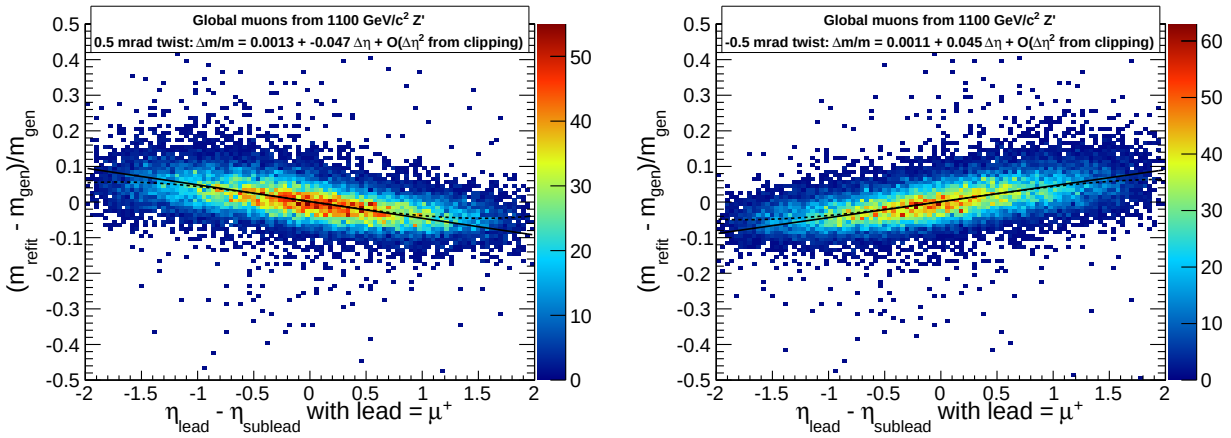

Figure 18: Same as Figs. 15 and 17 for opposite-direction twists.

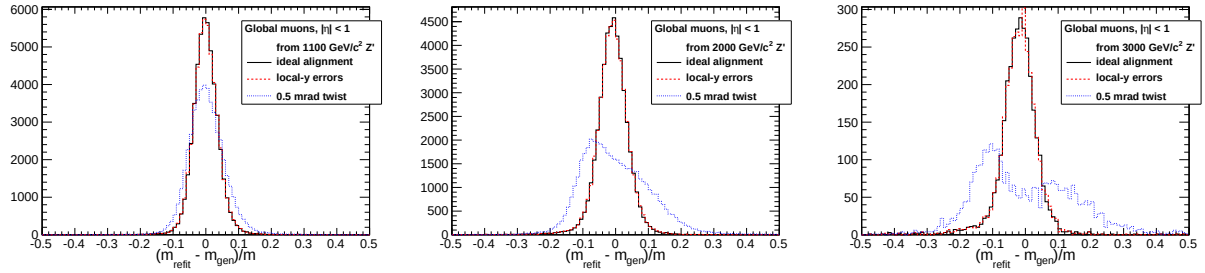

Figure 19: Mass resolution of Z' with ideal geometry (black), z-differences geometry (dashed red), and twist (dotted blue). Left is 1.1 TeV/c^2, middle is 2 TeV/c^2, and right is 3 TeV/c^2 and all three require $|\eta| < 1$ for both daughters. The z-differences geometry, affecting only the η of global tracks, has negligible effect on the Z' mass resolution. The effect of the twist geometry is significant and grows with Z' mass.

the uncertainty is dominated by muon momentum magnitudes, not directions. The twist has a significant effect on the mass resolution that grows with mass.

Improvement 5: this is where the "40%" figure comes from: the 1.1 TeV/c^2 Z' peak is deflated about 40% with respect to ideal geometry. How this compares with randomly but not systematically misaligned geometry has not yet been tested, but that would be more relevant than the 40% figure, since we really should be quantifying the difference between the best it might actually be and the worst it might actually be. We know that the geometry is not ideal.

Improvement 6: moreover, the $|\eta| < 1$ cut I apply not only gives an incomplete picture of the resolution, but it might not be tight enough to avoid the artificial effect of DT-CSC mismatch. The 3 TeV/c^2 Z' has a significantly different η distribution: it was less central than the 1.1 and 2 TeV/c^2 samples, which means that more of it samples the artificial smearing at $|\eta| \approx 1$. Actually, that sounds wrong, too: shouldn't higher-mass Z' bosons decay more centrally?

6 Conclusions

The main improvement is to include more than one effect: not just the barrel twist, but also how the endcap would follow the ends of the barrel. Many of the items labeled "improvement" above are different aspects of that one deficiency. Also, we will have systematic misalignment models of the endcap as well, and they should be included on an equal footing in the study. The "z-differences" test does not need to be repeated: it is irrelevant.

Ultimately, the only thing that is really needed is the 1-D mass resolution plot. However, I think that "monitoring" the effect as a function of kinematic variables shows that we have an understanding of the detector issues that cause it and we can be more confident that "x amount of misalignment uncertainty about some parameter yields y mass resolution smearing." I've already found most of the relevant variables: they can be added to an ntuple rather easily.